Quantification of Shoulder Joint Impedance during Dynamic Motion: A Pilot Study Using a Parallel-Actuated Shoulder Exoskeleton Robot

Seunghoon Hwang[1], Edward Chan[2], and Hyunglae Lee[1,*]

Abstract— **Previous studies characterizing shoulder joint impedance were either strictly limited to 2D planar motion or static postures in 3D space. It is still not clear how shoulder joint impedance is regulated during dynamic motion in 3D space. To address this knowledge gap, this study presents our initial efforts to quantify shoulder joint impedance during dynamic shoulder motion using a parallel-actuated shoulder exoskeleton robot. The robot's 4-bar spherical parallel manipulation mechanism, characterized by low inertia, allows for transparent and natural arm motion in 3D space and applies rapid perturbations to the upper arm during dynamic shoulder motion. Two unimpaired individuals participated in an experiment involving repeated shoulder flexion and extension motions at a fixed horizontal shoulder extension angle of 45°. Shoulder impedance was quantified by estimating the relationship between the kinematics of input perturbations, which were applied in the orthogonal direction of the arm motion, and the output torque responses resulting from these perturbations. This relationship was further approximated by a second-order model consisting of inertia, damping, and stiffness. Both subjects showed high reliability in impedance quantification during shoulder flexion and extension movements, evidenced by a high percentage Variance Accounted For that exceeds 96%. The experimental results showed the following notable trends. First, the contribution of stiffness to the shoulder torque was greater than that of the other two impedance parameters. Next, damping was larger during shoulder extension (downward motion) as opposed to flexion (upward motion). Lastly, inertia remained relatively constant regardless of shoulder motions. This pilot study validated the reliability of the presented robotic approach, paving the way for future shoulder impedance studies involving various dynamic motions in 3D space.**

I. INTRODUCTION

Many previous studies have demonstrated that the human neuromusculoskeletal system dynamically modulates the mechanical properties of limbs and joints during interactions with the surrounding mechanical environments [1], [2], [3]. These mechanical properties are commonly described by mechanical impedance, which is often further approximated by a second order system consisting of inertia, damping, and stiffness parameters [4].

Understanding and characterizing these properties in healthy individuals has important practical implications. The properties determined by mechanical impedance data can be used to further develop rehabilitation protocols for neurologically impaired patients who suffer from diminished joint mobility, and thus, improve clinical outcomes [5]. These properties could also contribute to enhancing the control systems of exoskeleton technology by replicating the dynamic and complex behaviors of human limbs and joints with greater precision [6].

In contrast to other human limbs and joints, shoulder joint impedance remains relatively unexplored, primarily due to its complex nature and the lack of suitable tools (e.g., robotic devices) for effective characterization. Previous studies on the shoulder joint have consequently focused on characterizing its impedance in a 2D horizontal plane under various task conditions [7], [8]. This was typically achieved using planar robotic systems, which initially characterized the endpoint impedance at the human hand and decomposed it into individual contributions from the elbow and shoulder joints through a Jacobian matrix. While these studies significantly contribute to our understanding of shoulder joint impedance and its role in planar motor tasks, they fall short in providing a comprehensive understanding of impedance regulation in 3D space.

There were several recent efforts to characterize shoulder joint impedance in 3D space. One study employed a servo motor and crank arm to directly apply position perturbations to the shoulder joint. This simple setup enabled the characterization of shoulder joint impedance across different arm postures and muscle contractions in 3D space [9], [10]. Another study utilized a forearm exoskeleton to provide perturbations in the horizontal abduction/adduction and internal/external directions of the shoulder [11]. Additionally, our previous study characterized the shoulder joint impedance under various arm postures in 3D space using a parallel-actuated shoulder exoskeleton robot [12], [13]. However, all of these characterizations were strictly limited to static postures.

This study aims to directly address this limitation by characterizing the shoulder joint impedance during dynamic motions in 3D space. As an initial step towards achieving this objective, a pilot study was conducted involving two healthy individuals. This study employed the same parallel-actuated shoulder exoskeleton robot used in our previous work characterizing the shoulder impedance during static posture maintenance tasks [12], [13].

The paper is structured as follows: Section II outlines the hardware setup used in the experiment, the experimental protocols, and the methods for data processing and analysis. Section III reports the outcomes of the human trials. Section IV discusses the implications of these findings and suggests avenues for future research.

S. Hwang and H. Lee are with the Neuromuscular Control and Human Robotics Laboratory, and School of Matter, Transport and Energy, Arizona State University, Tempe, AZ (email: {shwang45, hyunglae.lee}@asu.edu). , E. Chan is with the School of Biological and Health Systems Engineering, Arizona State University, Tempe, AZ (email:{echan9@asu.edu). *: corresponding author

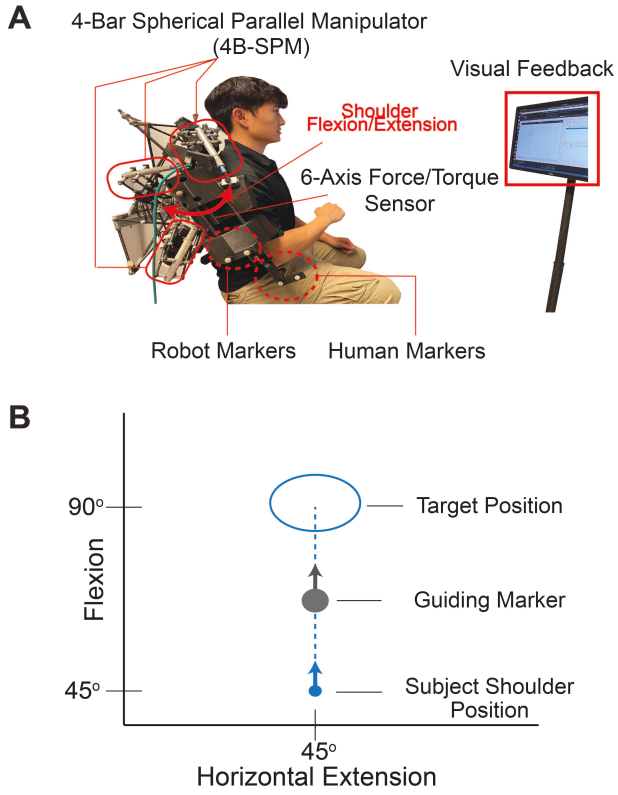

Fig. 1. (A): Experimental set up to characterize shoulder joint impedance during dynamic motion. (B): Visual feedback showing shoulder joint position, target position, and guiding marker.

II. Methods

A. Subjects

Two young, healthy individuals (2 males, age: 29 and 30 years, weight: 83 and 77 kg, and height: 166 and 168 cm) participated in this study, which was approved by the Institutional Review Board of Arizona State University (STUDY 00009059). The participants provided informed, written consent before participation. All experimental procedures were performed in accordance with the relevant guidelines and regulations.

B. Apparatus

In this study, a parallel-actuated shoulder exoskeleton robot, specifically a 4-bar spherical parallel manipulator (4B-SPM), was utilized to apply position perturbations directly to the subject's shoulder joint during dynamic motion tasks. The shoulder exoskeleton consists of three substructures, each equipped with two servo motors (Dynamixel MX-106R, Robotis, South Korea). These substructures work synergistically to actuate the end-effector of the shoulder exoskeleton, allowing the control of three rotational degrees-of-freedom in the shoulder joint with a large range of motion. This large range of motion enables the user to naturally move their arm in shoulder flexion-extension and horizontal flexion-extension directions. The robot's low end-effector inertia allows for the application of rapid position perturbations to the subject's shoulder joint, an essential aspect for the reliable quantification of shoulder joint impedance in 3D space [14], [15].

A 3D motion capture system (Bonita 10 System, Vicon, UK) was utilized to precisely track the movements of both the robot and the human subject. In parallel, a 6-axis force/torque (F/T) sensor (Axia 80 EDU, ATI-AI, NC, USA) was mounted on the end-effector plate of the exoskeleton to measure the torque at the shoulder joint. The integration of the exoskeleton with the subject was achieved through an upper arm cuff, which was connected to parallel carbon fiber rods positioned on the opposite side of the plate (as shown in Fig. 1A). This configuration ensures that the sensor's center is aligned with the rotational center of the end-effector, allowing for accurate measurement of the torque at the shoulder joint.

During movement tasks, visual feedback was provided to show the current angular position of the subject's shoulder joint and the target position that the subject was required to reach (Fig. 1B). Targets were set at 45 and 90° of shoulder flexion, with a constant horizontal extension maintained at 45°. To mitigate any effects of varying motion speeds across subjects, visual feedback included a guiding marker. When trials started, this marker moved to the target position in flexion and extension at a constant speed of 0.4 rad/s, and subjects were instructed to follow this guiding marker as they moved towards the target.

An admittance controller was employed for interaction control, ensuring transparent and natural movement for the subject when using the shoulder exoskeleton robot during dynamic motion tasks. This controller switched to position control mode instantaneously (within 4 ms) when applying perturbations to the subject's shoulder joint.

C. Experiment protocol

Prior to the main experiment, the maximum voluntary contraction (MVC) of three major shoulder muscles — specifically the anterior deltoid (AD), medial deltoid (MD), and posterior deltoid (PD) — was measured. This was done to analyze how the shoulder muscles are activated during dynamic arm motion.

The main experiment was organized into 10 blocks, each consisting of 5 trials with perturbations and 5 trials without perturbations. During each trial, the subject moved their arm to a target position indicated by visual feedback. The goal position was set at 45° when the arm was moved in the extension direction, and at 90° when moved in the flexion direction. Subjects were instructed to track the guiding marker with continuous movement without stopping before they reached the target position.

In the perturbation trials, ramp perturbations with an 8° magnitude were applied to the subject's shoulder joint in the orthogonal direction to the subject's movement, specifically in the horizontal extension direction. These perturbations were applied randomly at 65-70° of shoulder flexion. The trials were randomly assigned and consisted of 50 perturbation trials and 50 unperturbed trials, distributed across a total of 10 blocks. The perturbation trials were evenly distributed,

with 25 trials occurring when the arm was moving in the flexion direction and 25 trials in the extension direction. A 2-3 minute break was provided between each block to prevent potential fatigue effects on the results.

D. Data Processing and Analysis

Shoulder position and torque data were measured using the motion capture system and F/T sensor, with the sampling rate set at 250 Hz. Additionally, all measured data were filtered using a 4th-order Butterworth low-pass filter with a cutoff frequency of 10 Hz.

For the quantification of shoulder joint impedance using perturbations, the position and torque measurements from the unperturbed trials were averaged and then subtracted from those in the perturbation trials. Additionally, to adjust the position and torque offset in the perturbation trials, the average position and torque values within a time window of 200 ms preceding each perturbation were subtracted. For calculating the velocity and acceleration profiles, a 5-point central numerical differentiation method was employed. The time window for impedance analysis was determined by averaging the timing of peak torque across all perturbation trials for each subject. For the quantification of shoulder joint impedance using perturbations, the position and torque measurements from the unperturbed trials were averaged and then subtracted from those in the perturbation trials. Additionally, to adjust the position and torque offset in the perturbation trials, the average position and torque values within a time window of 200 ms preceding each perturbation were subtracted. For calculating the velocity and acceleration profiles, a 5-point central numerical differentiation method was employed. The time window for impedance analysis was determined by averaging the timing of peak torque across all perturbation trials for each subject.

The shoulder joint impedance was estimated using a second-order parametric model and a constrained optimization technique that employed the Levenburg-Marquardt nonlinear least squares method [16]. Constraints were set to ensure that both stiffness and damping values were non-negative. A lower bound for inertia was established based on the subject's arm weight, which was set to be 5% of the subject's body weight [17], and the moment arm measured as the distance between the center of the shoulder joint and the arm interface.

To estimate the variability in the quantification of shoulder impedance and to conduct statistical analysis on each subject's data, bootstrapping was utilized. This involved repeatedly sampling, 100 times, with replacement from the original data set. The sampling process continued until it encompassed 70% of the total perturbation trials. After reaching this threshold, the sampled data were averaged.

The reliability of the impedance quantification was evaluated by calculating the percentage Variance Accounted For (%VAF) between the measured torque and the estimated torque using the estimated impedance parameters, i.e., inertia, damping, and stiffness.

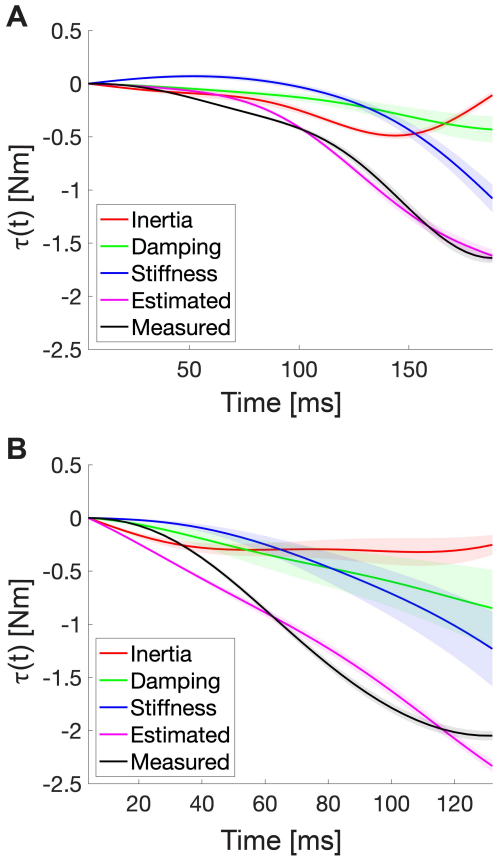

Fig. 2. The torque profiles for a sample subject during flexion motion (A) and extension motion (B). The contributions to the torque from inertia, damping, stiffness are represented by red, green, and blue lines, respectively. The measured torque (black) aligns closely with the estimated torque, which is obtained by summing the contributions from the three impedance parameters (magenta). The bold line represents the mean, while the shaded area indicates the mean ±1 standard deviation.

To investigate any statistical differences in each subject's impedance parameters between shoulder flexion and extension movement trials, paired sampled t-test were performed for each subject's bootstrapped data sets with an independent variable of shoulder movement direction and dependent variables of the three impedance parameters. Statistical analyses were performed using SPSS (v28, IBM, USA) at a significance level of 0.05.

III. Results

The experimental results demonstrated a high level of reliability in quantifying shoulder joint impedance during dynamic movements. This is evidenced by the high %VAF for both shoulder flexion and extension movements in the results of both subjects, which exceeded 96% (Table I). The torque plots for a sample subject indicate a good alignment between the estimated torque (magenta) — accounting for torque generated by inertia, damping, and stiffness — and the measured torque (black) during both shoulder flexion and extension trials (Fig. 2). Initially, inertia dominated the overall torque response, but the contribution of stiffness gradually increased in the later phase of the perturbation.

TABLE I

SUMMARY OF SHOULDER IMPEDANCE QUANTIFICATION DURING DYNAMIC MOTION IN FLEXION AND EXTENSION DIRECTIONS.

Flexion direction	I (kgm^2)	B (Nms/rad)	K (Nm/rad)	VAF (%)	I contribution (%)	B contribution (%)	K contribution (%)
Subject 1	0.14 (0.0003)	0.4 (0.2)	69.8 (0.5)	97.3 (0.9)	28.0 (3.5)	12.0 (4.6)	60.0 (3.5)
Subject 2	0.11 (4.3E^{-9})	0.9 (0.2)	41.8 (4.4)	98.8 (0.5)	35.2 (4.0)	27.7 (7.0)	37.1 (4.9)
Extension direction	I (kgm^2)	B (Nms/rad)	K (Nm/rad)	VAF (%)	I contribution (%)	B contribution (%)	K contribution (%)
Subject 1	0.14 (0.0003)	0.8 (0.3)	55.9 (5.4)	96.5 (0.8)	39.7 (1.7)	14.2 (4.6)	46.0 (4.7)
Subject 2	0.11 (0.001)	1.8 (0.6)	45.3 (7.9)	96.2 (0.7)	24.1 (5.2)	33.3 (10.2)	42.6 (9.9)

The results are reported as mean (standard deviation).

TABLE II

MUSCLE ACTIVATION LEVEL DURING PERTURBATION TRIALS

Flexion direction	AD	MD	PD
Subject 1	9.8 (0.5)	5.5 (0.6)	0.5(0.1)
Subject 2	11.6 (0.6)	5.4 (0.6)	0.7 (0.02)
Extension direction	AD	MD	PD
Subject 1	6.2 (0.9)	4.9 (0.8)	1.3 (0.1)
Subject 2	9.9 (0.1)	3.5 (0.3)	0.8 (0.01)

* Muscle activation prior to the perturbations (200 ms window) is reported in %MVC.

The estimated stiffness results showed differences between Subject 1 and Subject 2. Subject 1 exhibited higher shoulder joint stiffness during flexion motion (69.8 Nm/rad) compared to extension motion (55.9 Nm/rad). In contrast, Subject 2 demonstrated slightly greater stiffness during shoulder extension motion (45.3 Nm/rad) than during flexion motion (41.8 Nm/rad). The results of paired t-tests indicated that the direction of shoulder movement significantly affects shoulder joint stiffness in both Subject 1 ($p < 0.001$) and Subject 2 ($p = 0.007$). In addition, the contribution of shoulder stiffness to the generation of overall shoulder torque was consistently larger than that of damping and inertia for both subjects, with an average contribution of 48.6% and 44.3% during shoulder flexion and extension motions, respectively.

The estimated damping results showed the same trend in both subjects. During extension motion, the damping values were 0.8 and 1.8 Nms/rad for Subjects 1 and 2, respectively. In contrast, for shoulder flexion motion, lower damping values of 0.4 and 0.9 Nms/rad were observed. This suggests that damping during shoulder extension motion is approximately twice that during flexion motion. The results of paired t-tests showed a significant effect of shoulder movement direction on damping for both Subject 1 ($p < 0.001$) and Subject 2 ($p < 0.001$). Additionally, the contribution of shoulder damping to the overall shoulder torque was about 20% higher during shoulder extension motion than during flexion motion. The inertia remained largely constant, irrespective of the direction of movement, showing very low variability in inertia estimation. The statistical analysis results indicated no significant difference in inertia for both Subject 1 ($p = 0.58$) and Subject 2 ($p = 0.08$).

During shoulder flexion and extension movements, while maintaining a constant horizontal extension angle at 45°, both subjects showed relatively higher AD and MD activation compared to PD activation (Table II).

IV. DISCUSSION

This study aimed to address the limitations of previous studies that characterized shoulder joint impedance in either 2D planar motion or static postures in 3D space. The 4B-SPM shoulder exoskeleton robot, which has low end-effector inertia and allows for transparent and natural shoulder motion over a large range of motion, enabled the reliable quantification of shoulder joint impedance during dynamic motion, specifically in the shoulder flexion and extension directions.

A pilot study involving two young, healthy individuals demonstrated that the shoulder joint impedance can be accurately approximated as a second-order system consisting of stiffness, damping, and inertia (%VAF $>$ 96%). This finding is consistent with previous studies that characterized other joint impedance during dynamic motion [18], as well as studies focusing on shoulder joint impedance during static postures [10], [13]. Each subject showed different patterns of stiffness modulations during shoulder flexion and extension movements. Subject 1 exhibited higher stiffness during flexion than during extension, which could be partly explained by higher AD activation during this motion. While statistically significant, Subject 2 exhibited a smaller difference in stiffness between the two movement directions. Both subjects exhibited significantly higher damping during extension motion. However, given the limited number of subjects in this pilot study, further studies with a larger group of subjects seem warranted to clearly understand the effects of shoulder movement direction on both stiffness and damping.

For future studies, we plan to extend our research to encompass a wider range of shoulder motion in 3D space. Furthermore, we aim to compare shoulder joint impedance during static postures and dynamic movement. This comparison will advance our scientific understanding of how the human neuromuscular system modulates shoulder joint impedance depending on the type of motor tasks.

ACKNOWLEDGMENT

This work was supported by National Science Foundation Awards 1846885 and 1925110.

REFERENCES

[1] S. Richter, P. Jansen-Osmann, J. Konczak, and K.-T. Kalveram, "Motor adaptation to different dynamic environments is facilitated by indicative context stimuli," *Psychological Research*, vol. 68, no. 4, pp. 245–251, 2004.

[2] A. C. Schouten, E. De Vlugt, J. Van Hilten, and F. C. Van Der Helm, "Quantifying proprioceptive reflexes during position control of the human arm," *IEEE Transactions on Biomedical Engineering*, vol. 55, no. 1, pp. 311–321, 2007.

[3] A. Needle, J. Baumeister, T. Kaminski, J. Higginson, W. Farquhar, and C. Swanik, "Neuromechanical coupling in the regulation of muscle tone and joint stiffness," *Scandinavian journal of medicine & science in sports*, vol. 24, no. 5, pp. 737–748, 2014.

[4] N. Hogan, "Mechanical impedance of single-and multi-articular systems," in *Multiple muscle systems: Biomechanics and movement organization*. Springer, 1990, pp. 149–164.

[5] F. Buma, G. Kwakkel, and N. Ramsey, "Understanding upper limb recovery after stroke," *Restorative neurology and neuroscience*, vol. 31, no. 6, pp. 707–722, 2013.

[6] H. Lee and N. Hogan, "Essential considerations for design and control of human-interactive robots," in *2016 IEEE International Conference on Robotics and Automation (ICRA)*. IEEE, 2016, pp. 3069–3074.

[7] H. Gomi and M. Kawato, "Human arm stiffness and equilibrium-point trajectory during multi-joint movement," *Biological cybernetics*, vol. 76, no. 3, pp. 163–171, 1997.

[8] E. J. Perreault, R. F. Kirsch, and P. E. Crago, "Multijoint dynamics and postural stability of the human arm," *Experimental brain research*, vol. 157, no. 4, pp. 507–517, 2004.

[9] B. J. Diefenbach and D. B. Lipps, "Postural differences in shoulder dynamics during pushing and pulling," *Journal of biomechanics*, vol. 85, pp. 67–73, 2019.

[10] D. B. Lipps, E. M. Baillargeon, D. Ludvig, and E. J. Perreault, "Quantifying the multidimensional impedance of the shoulder during volitional contractions," *Annals of biomedical engineering*, vol. 48, pp. 2354–2369, 2020.

[11] Y. Z. Yahya, I. W. Hunter, T. F. Besier, A. J. Taberner, and B. P. Ruddy, "Shoulder joint stiffness in a functional posture at various levels of muscle activation," *IEEE Transactions on Biomedical Engineering*, vol. 69, no. 7, pp. 2192–2201, 2021.

[12] D. Chang, J. Hunt, J. Atkins, and H. Lee, "Validation of a novel parallel-actuated shoulder exoskeleton robot for the characterization of human shoulder impedance," in *2021 IEEE International Conference on Robotics and Automation (ICRA)*. IEEE, 2021, pp. 10 580–10 586.

[13] S. Hwang, A. Saxena, E. Oleen, S. L. Paing, J. Atkins, H. Lee *et al.*, "Characterization of human shoulder joint stiffness across 3d arm postures and its sex differences," *Authorea Preprints*, 2023.

[14] J. Hunt and H. Lee, "A new parallel actuated architecture for exoskeleton applications involving multiple degree-of-freedom biological joints," *Journal of Mechanisms and Robotics*, vol. 10, no. 5, p. 051017, 2018.

[15] J. Hunt and H. Lee, "Development of a low inertia parallel actuated shoulder exoskeleton robot for the characterization of neuromuscular property during static posture and dynamic movement," in *2019 International Conference on Robotics and Automation (ICRA)*. IEEE, 2019, pp. 556–562.

[16] R. E. Kearney, R. B. Stein, and L. Parameswaran, "Identification of intrinsic and reflex contributions to human ankle stiffness dynamics," *IEEE transactions on Biomedical Engineering*, vol. 44, no. 6, pp. 493–504, 1997.

[17] S. Plagenhoef, F. G. Evans, and T. Abdelnour, "Anatomical data for analyzing human motion," *Research quarterly for exercise and sport*, vol. 54, no. 2, pp. 169–178, 1983.

[18] H. Lee, E. J. Rouse, and H. I. Krebs, "Summary of human ankle mechanical impedance during walking," *IEEE journal of translational engineering in health and medicine*, vol. 4, pp. 1–7, 2016.